Structural and Bonding Trends in Platinum−Carbon Clusters

Thomas F. Miller III and Michael B. Hall*

Contribution from the Department of Chemistry, Texas A&M University, College Station, Texas 77843-3255

Received March 17, 1999. Revised Manuscript Received June 9, 1999

Abstract: Density functional calculations with the B3-LYP functional were used to optimize the platinum−carbon cationic clusters, PtC_x^+, $1 \le x \le 16$, in both the doublet and quartet states of the linear, fan, open-ring, closed-ring, and one-carbon-ring geometries. Trends in stability, Pt^+-C_x binding energy, doublet-quartet excitation energy, and Pt−C bond lengths were investigated. Explanations for these patterns are provided in terms of orbital interactions and changes imposed on the carbon chain by the metal atom. In accord with the previously studied palladium−carbon cations, the PtC_x^+ clusters favored a linear geometry for $3 \le x \le 9$. For larger clusters, the open-ring (Pt inserted in C_x ring) and closed-ring (Pt bound to two atoms of closed C_x ring) families exhibit the lowest-energy structures. The stability and the nature of the Pt−C bonding in both the closed-ring and one-carbon-ring (Pt bound to one atom of closed C_x ring) PtC_x^+ structures depend greatly on the aromaticity of the corresponding C_x ring. However, unlike their palladium counterparts, the closed-ring platinum clusters were found invariably to be more stable than the respective one-carbon species. The stability of forming two Pt−C σ bonds is due to relatively lower energy sd hybrid orbitals from the platinum cation.

Introduction

Since the much heralded discovery of buckminsterfullerene in 1985,[1,2] there has been considerable interest in both neutral and ionic small carbon clusters. Not only are these clusters likely to serve as precursors to larger fullerene complexes[3−7] but also their manageable size makes them suitable for high-precision theoretical and experimental analysis.[7−14] Although the electronic complexity of these C_x clusters has long hindered the conclusive identification of their structural trends, the recent utilization of advanced theoretical techniques has led to significant progress.[15−25] Controversies have arisen regarding the sensitivity of predicted geometries to the method of calculation,[19−26] but it is generally accepted that monocyclic ring conformations are favorable to linear conformations for $x > 9$.[7,17,21,23,24] In addition, evidence exists to suggest that, for clusters with $x > 14$, both the linear structures and monocyclic rings are suspected to transform from the cumulene-like geometries (equal C−C bond lengths) expected for fewer carbon atoms to those more akin to polyacetylenes (significant bond length alternations).[17,20,22,23]

More recently, the ion-mobility studies of Jarrold[27−30] have identified the binding of a single transition metal cation to a variety of carbon clusters. However, the nature of this interaction is still unclear because only a very qualitative picture of a compound's structural properties can be derived from ion-mobility experiments. By measuring the rate at which a molecule proceeds through an inert gas-filled drift tube, ion mobility provides the effective collisional cross-section of the molecules in question. This collisional cross-section only indicates the compactness of a complex's geometry, neglecting its more subtle qualities.[31,32] Several theoretical investigations have succeeded in clarifying the structural conclusions that can be drawn from the experimental work.[33−35] These studies have shown that, for

(1) Kroto, H. W.; Heath, J. F.; O'Brien, S. C.; Curl, R. F.; Smalley, R. E. *Nature* **1985**, *318*, 162.
(2) Zhang, Q. L.; O'Brien, S. C.; Heath, J. R.; Liu, Y.; Curl, R. F.; Kroto, H. W.; Smalley, R. E. *J. Phys. Chem.* **1986**, *90*, 525.
(3) Wang, Z. L.; Kang, Z. C. *J. Phys. Chem.* **1996**, *100*, 17725.
(4) von Helden, G.; Hsu, M. T.; Gotts, N.; Bowers, M. T. *J. Phys. Chem.* **1993**, *97*, 8182.
(5) Hunter, J. M.; Fye, J. L.; Roskamp, E. J.; Jarrold, M. F. *J. Phys. Chem.* **1994**, *98*, 1810.
(6) Hunter, J. M.; Jarrold, M. F. *J. Am. Chem. Soc.* **1995**, *117*, 10317.
(7) Weltner, W., Jr.; van Zee, R. J. *Chem. Rev.* **1989**, *89*, 1713.
(8) Taylor, P. R.; Martin, J. M. L.; Francois, J. P.; Gijbels, R. *J. Phys. Chem.* **1991**, *95*, 6530.
(9) Watts, J. D.; Bartlett, R. J. *J. Chem. Phys.* **1992**, *96*, 6073.
(10) Sommerfeld, T.; Scheller, M. K.; Cederbaum, L. S. *J. Phys. Chem.* **1994**, *98*, 8914.
(11) Sowa-Resat, M. B.; Hintz, P. A.; Anderson, S. L. *J. Phys. Chem.* **1995**, *99*, 10736.
(12) Forney, D.; Grutter, M.; Freivogel, P.; Maier, J. P. *J. Phys. Chem.* **1997**, *101*, 5292.
(13) Wang, X. B.; Ding, C. F.; Wang, L. S. *J. Phys. Chem.* **1997**, *101*, 7699.
(14) Szczepanski, J.; Auerbach, E.; Vala, M. *J. Phys. Chem.* **1997**, *101*, 9296.
(15) Martin, J. M. L.; Taylor, P. R. *J. Phys Chem.* **1996**, *100*, 6047.
(16) Watts, J. D.; Bartlett, R. J. *J. Chem. Phys.* **1992**, *97*, 3445.
(17) Liang, C.; Schaefer, H. F., III *J. Chem. Phys.* **1990**, *93*, 8844.
(18) Parasuk, V.; Almlof, J. *J. Chem. Phys.* **1989**, *91*, 1137.
(19) Parasuk, V.; Almlof, J.; Feyereisen, M. W. *J. Am. Chem. Soc.* **1991**, *113*, 1049.
(20) Plattner, D. A.; Houk, K. N. *J. Am. Chem. Soc.* **1995**, *117*, 4405.
(21) Hutter, J.; Luthi, H. P.; Diederich, F. *J. Am. Chem. Soc.* **1994**, *116*, 750.
(22) Liang, C.; Schaefer, H. F., III *Chem. Phys. Lett.* **1990**, *169*, 150.
(23) Watts, J. D.; Bartlett, R. J. *Chem. Phys. Lett.* **1992**, *190*, 19.
(24) Martin, J. M. L.; Taylor, P. R. *J. Phys. Chem.* **1996**, *100*, 6047.
(25) Grossman, J. C.; Mitas, L.; Raghavachari, K. *Phys. Rev. Lett.* **1995**, *75*, 3870.
(26) Raghavachari, K.; Strout, D. L.; Odom, G. K.; Scuseria, G. E.; Pople, J. A.; Johnson, B. G.; Gill, P. M. W. *Chem. Phys. Lett.* **1993**, *214*, 357.
(27) Shelimov, K. B.; Jarrold, M. F. *J. Phys. Chem.* **1995**, *99*, 17677.
(28) Shelimov, K. B.; Clemmer, D. E.; Jarrold, M. F. *J. Phys. Chem.* **1995**, *99*, 11376.
(29) Clemmer, D. E.; Jarrold, M. F. *J. Am. Chem. Soc.* **1995**, *117*, 8841.
(30) Shelimov, K. B.; Jarrold, M. F. *J. Am. Chem. Soc.* **1996**, *118*, 1139.
(31) Strout, D. L.; Book, L. D.; Millam, J. M.; Xu, C.; Scuseria, G. E. *J. Phys. Chem.* **1994**, *98*, 8622.
(32) Book, L. D.; Millam, J. M.; Xu, C.; Scuseria, G. E. *Chem. Phys. Lett.* **1994**, *222*, 281.
(33) Strout, D. L.; Hall, M. B. *J. Phys. Chem.* **1996**, *100*, 18007.
(34) Strout, D. L.; Hall, M. B. *J. Phys. Chem. A* **1998**, *102*, 641.

10.1021/ja990854n CCC: $18.00
Published on Web 08/03/1999

similar complexes, a few basic structural families encompass the most stable geometries for $x \leq 16$:

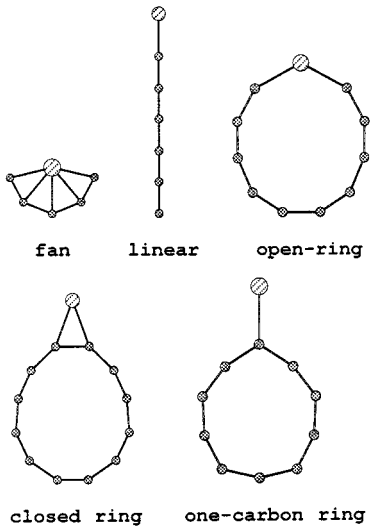

However, little is known about the transition metal−carbon bonding or the molecular electronic patterns exhibited by these clusters.

We have calculated the energies, orbital occupations, and optimal geometries of the doublet and quartet states of PtC_x^+, $1 \leq x \leq 16$. Among those quantities investigated will be stability, Pt^+-C_x binding energy, doublet-quartet excitation energy, and trends in Pt−C bond lengths. In addition, explanations for these phenomena will be provided from analysis of the orbital interactions and changes imposed on the carbon chain by the metal atom.

Theoretical Methods

All calculations in this work were performed with the Gaussian 94 program.[36] Geometry optimizations and energy calculations were carried out using the B3-LYP density functional method, which includes the Becke[37] three-parameter (B3) exchange functional and the Lee−Yang−Parr[38] (LYP) correlation functional. All calculations included the relativistic effective core potential of Hay and Wadt[39] for the platinum atoms. The basis set used was the Huzinage−Dunning[39] double-ζ basis set for the carbon atoms and the double-ζ basis set of Hay and Wadt[42] for the platinum atoms. In the platinum basis, the two outermost p-functions were replaced by a (41) split of the optimized outer p-function from Couty and Hall.[41]

As discussed by Plattner et al.,[20] a number of density functional theory (DFT) functionals (namely, B-LYP, B3-LYP, and LSDA) tend to favor cumulene-like geometries for large C_x clusters, contrary to the tendency of Hartree−Fock (HF) theory[42] to prefer localized, polyacetylene-like configurations. However, the utilization of a method containing electron correlation improves the geometric results,[23,25] and DFT more closely reproduces the results obtained from post-HF methods such as CCSD(T) for small C_x clusters.[24] Also, the B3-LYP functional is among the most reliable DFT functionals, consistently generating better results than those obtained from both the LDA method and B-LYP functional.[20,25,26,34] Thus, it appears safe to assume that the B3-LYP functional will give satisfactory results for these complexes and DFT will suffice as the employed method.

Also, the relatively small double-ζ basis set for the carbon atoms presents a limitation to the numerical accuracy of these calculations. In particular, ring strain in the compounds will be exaggerated to varying degrees. However, because the smallest cyclic carbon chains analyzed in this study are six-membered, many of the worst cases of ring strain overestimation are not included.

Another possible concern is the use of the Kohn−Sham orbitals from the DFT calculations to analyze the bonding in the PtC_x^+ systems. Although Kohn−Sham orbitals are not equivalent to those obtained from a pure wave function method, it will be assumed that the differences are minor enough to bear no significance on the qualitative arguments put forth in this study.

In concurrence with the theoretical and experimental analysis of related M_xC_y species,[21,43] we found that a number of the cyclic PtC_x^+ clusters underwent slight distortions from C_{2v} symmetry, the highest possible symmetry for monocyclic clusters with an externally bound metal atom. However, these slight geometric aberrations did not seem to be accompanied by significant alterations in energy or electronic structure. Thus, as in previous studies,[33−35] all cyclic complexes were optimized and analyzed in the full C_{2v} point group.

Table 1. Relative Stablility of the Linear and Fan Structures in the Doublet States

carbon atoms	(doublet linear − doublet fan) (kcal mol^{-1})
2	3.98
3	−57.1
4	−51.5
5	−83.7

Results

Small Clusters. As seen in Table 1, the fan structures for $x \geq 3$ were all highly unstable with respect to the linear PtC_x^+ complexes. A fanlike geometry is found to be competitive only for the case of $x = 2$. The two equivalent Pt−C bonds in the PtC_2^+ fan are formed from the interaction of the carbon orbitals with sd hybrid orbitals on the platinum cation. The low energy of the 6s platinum orbital makes possible this hybridization and leads to the stability of the molecule. Larger clusters were investigated in which the platinum atom bridges the first two carbons of an essentially linear C_x chain, but all optimized to the totally linear geometry.

These results are in contrast to the calculations[33,34] for the early transition metal compounds LaC_x^+ and YC_x^+, in which the fan structure was consistently favored. However, with the electron-rich d^9 ground state for Pt^+, the formation of more than two σ bonds would require the utilization of numerous unoccupied orbitals on the small C_x moiety.

Linear Clusters. Figure 1 and Table 2 display the binding energies and platinum−carbon bond lengths, respectively, for the doublet and quartet states of each calculated linear cluster. The binding energy was determined by subtracting the total energy of each PtC_x^+ system from the calculated energies of the Pt^+ cation in the ^2D state and the respective ground-state C_x chain. In general, the PtC_x^+ systems with even values of x have energetically competitive doublet and quartet states. For even values of x, the doublet states exhibit platinum−carbon

(35) Strout, D. L.; Miller, T. F., III; Hall, M. B. *J. Phys. Chem. A* **1998**, *102*, 6307.
(36) Frisch, M. J.; Trucks, G. W.; Schlegel, H. B.; Gill, P. M. W.; Johnson, B. G.; Robb, M. A.; Cheeseman, J. R.; Keith, T.; Petersson, G. A.; Montgomery, J. A.; Raghavachari, K.; Al-Laham, M. A.; Zakrzewski, V. G.; Ortiz, J. V.; Foresman, J. B.; Cioslowski, J.; Stefanov, B. B.; Nanayakkara, A.; Challacombe, M.; Peng, C. Y.; Ayala, P. Y.; Chen, W.; Wong, M. W.; Andres, J. L.; Replogle, E. S.; Gomperts, R.; Martin, R. L.; Fox, D. J.; Binkley, J. S.; Defrees, D. J.; Baker, J.; Stewart, J. P.; Head-Gordon, M.; Gonzalez, C.; Pople, J. A. *Gaussian 94*, Revision D.4; Gaussian, Inc.: Pittsburgh, PA, 1995.
(37) Becke, A. D. *J. Chem. Phys.* **1993**, *98*, 5648.
(38) Lee, C.; Yang, W.; Parr, R. G. *Phys. Rev. B* **1988**, *37*, 785.
(39) Dunning, T. H.; Hay, P. J. *Modern Theoretical Chemistry*; Schaefer, H. F., III, Ed.; Plenum: New York, 1976; pp 1−28.
(40) Hay, P. J.; Wadt, W. R. *J. Chem. Phys.* **1985**, *82*, 299.
(41) Couty, M.; Hall, M. B. *J. Comput. Chem.* **1996**, *17*, 1359.
(42) Roothaan, C. C. *Rev. Mod. Phys.* **1951**, *23*, 69.
(43) Rubin, Y.; Knobler, C. B.; Diederich, F. *J. Am. Chem. Soc.* **1990**, *112*, 4966.

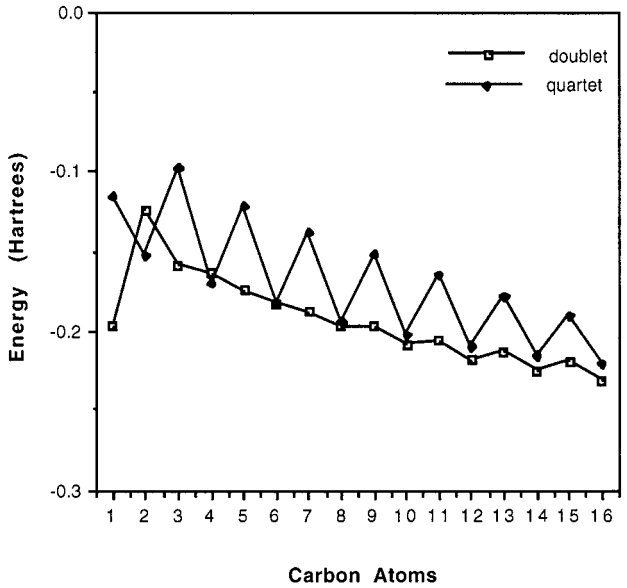

Figure 1. The binding energy of the doublet and quartet states of the linear PtC_x^+ clusters with respect to Pt^+ and the corresponding linear C_x chain.

Table 2. Pt−C Bond Length in the Doublet and Quartet States of the Linear and Open-Ring PtC_x^+ Clusters

	linear (Å)		open-ring (Å)	
x	doublet	quartet	doublet	quartet
1	1.72	1.88		
2	1.76	1.80		
3	1.84	1.84		
4	1.76	1.85		
5	1.85	1.85		
6	1.76	1.86	1.87	1.93
7	1.86	1.86	1.88	1.93
8	1.76	1.86	1.88	1.94
9	1.86	1.86	1.90	1.88
10	1.77	1.86	1.87	1.90
11	1.87	1.86	1.87	1.92
12	1.77	1.87	1.87	1.93
13	1.87	1.78	1.90	1.88
14	1.77	1.87	1.87	1.89
15	1.77	1.78	1.87	1.91
16	1.77	1.87	1.87	1.92

bond lengths of 1.76−1.77 Å, while the quartet states exhibit considerably longer values at about 1.86 Å. In cases of odd x, the doublet state is invariably more stable. Also, for odd $x \leq 11$, little difference is found in the platinum−carbon bond lengths of the doublet and quartet states. With larger values of x, however, the bond length in both states shortens dramatically from approximately 1.86 Å to approximately 1.78 Å. In the quartet state, this contraction of the Pt−C bond occurs at $x = 13$, whereas it occurs at $x = 15$ in the doublet state. To understand these trends, we will describe the bonding of the bare C_x chains and then the nature of the Pt^+ interaction with these chains.

First consider the orbitals of the linear C_x chains. Our calculations of these carbon clusters are in accord with the results from previous experimental and theoretical work.[17,18,21,22] We found $^1\Sigma_g^+$ to be the ground state for carbon chains with odd values of x and $^3\Sigma_g^-$ to be the ground state for even $x > 2$. Our only discrepancy from previous experimental[3] work is for $x = 2$ in which the $^1\Sigma_g^+$ state has been observed to be more stable than the lowest triplet state ($^3\Pi_u$) by 716 cm^{-1}. Our calculations found the lowest-energy triplet (unrestricted single determinant) to be favored over the $^1\Sigma_g^+$ state by 6966 cm^{-1}. Previous studies

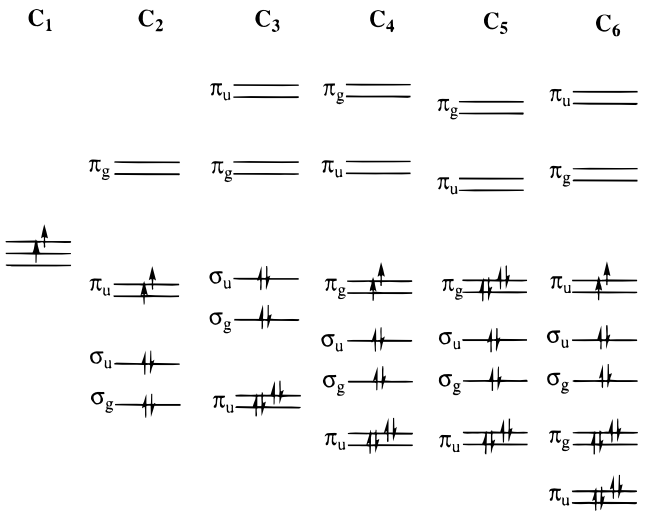

Figure 2. Partial MO diagram showing the orbitals in the frontier region of the linear C_x chains.

using DFT[21] have noted the same problem. Fortunately, this small anomaly exists only for the case of $x = 2$.

Figure 2 is a partial molecular orbital diagram showing the terminal lone pairs and lowest π molecular orbitals for C_x, $1 \leq x \leq 6$. For $x \geq 2$, the frontier orbitals of even and odd x have very characteristic properties. For all cases, the frontier orbitals exhibit two filled lone pairs of σ symmetry (σ_g and σ_u) and two sets of unoccupied π orbitals (except for $x = 2$, which only has one set). Also, the cases with even x exhibit a degenerate pair of singly occupied π orbitals (alternately π_g and π_u), while the cases with odd x have a set of completely filled π orbitals (alternately π_g and π_u).

Figure 2 shows that, although the HOMO was of σ symmetry for $x = 3$, the C_5 linear cluster has a π HOMO. This change in the order of orbital energies with increasing chain length may be described in numerous ways. For the sake of consistency in subsequent explanations, we shall consider the previously existing π orbitals to have risen in energy with respect to the σ orbitals. Such an occurrence is not at all unexpected. As the carbon chain grows in length, the occupied π molecular orbitals will form a continuum or band. That is, increasing numbers of π orbitals will be found around the HOMO−LUMO gap, eventually converging at the Fermi level. This phenomenon will manifest itself in Figure 2 by the relative destabilization of pairs of occupied π orbitals with respect to the σ lone pairs. As another example, beginning at $x = 12$, a second pair of π orbitals (completely occupied) becomes less stable than the σ lone pairs for the clusters with even x. Thus, at $x = 13$, two pairs of totally occupied π orbitals are less stable than the σ lone pairs. (Recall that the first occurred at $x = 5$ for the linear clusters with odd x.)

An understanding of the bonding in linear PtC_x^+ clusters can be obtained by considering the interaction of the 5d and 6s orbitals of the metal ion with the prescribed frontier orbitals of the respective C_x cluster. Figures 3, 4, and 5 are partial molecular orbital diagrams of linear PtC_x^+ clusters with $x = 1$, $x = 2n + 1$, and $x = 2n$, respectively. In each, the 5d and 6s orbitals from Pt^+ on the left are shown to interact with orbitals from various C_x chains on the right. These diagrams will be utilized in the following discussion.

PtC^+. Consider first the special case of $x = 1$ (Figure 3). A close examination of this diagram is worthwhile because it contains many of the essential elements of the more complicated Figures 4 and 5. Clearly, the δ orbitals of Pt^+ are nonbonding

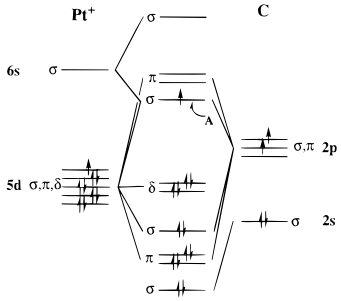

Figure 3. Partial MO diagram showing the interaction of the platinum cation and a single carbon atom.

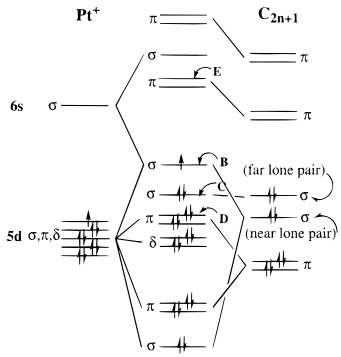

Figure 4. Partial MO diagram showing the interaction of the platinum cation and a linear carbon cluster of odd chain length.

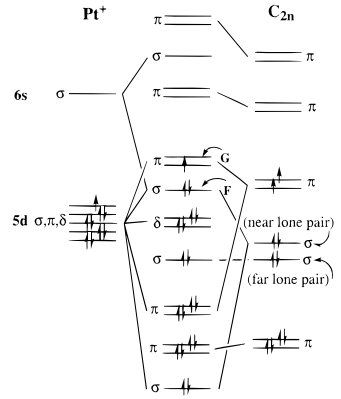

Figure 5. Partial MO diagram showing the interaction of the platinum cation and a linear carbon cluster of even chain length.

because of the lack of available orbitals of the same symmetry on the carbon atom. Three significant bonding interactions are found at energies below that of the δ orbitals. The 5d orbitals from Pt^+ and the 2s and 2p orbitals from the carbon atom interact to form a σ bond, a pair of π bonds, and a carbon lone pair of σ symmetry. Orbital A, which is found at higher energy than the nonbonding δ orbitals, would at first glance appear to be strongly antibonding. However, we will see that its strong interaction with the 6s orbital from Pt^+ diminishes this antibonding character.

It is clearly seen from Figure 1 and Table 2 that the nature of the Pt−C bond in the doublet state of PtC^+ is unique among the complexes examined. Both the reduced bond length and the increased binding energy indicate a very strong metal−carbon interaction. Interestingly, the neutral PtC complex, which exhibits the double-occupation of orbital A in Figure 3, is calculated to have a Pt−C bond length within 0.003 Å of that found in PtC^+. This constant Pt−C bond length implies that orbital A is essentially nonbonding, allowing both PtC and PtC^+ to exhibit triple-bond character. The anticipated antibonding character in orbital A is essentially eliminated by its stabilizing interaction with the low-lying Pt^+ 6s orbital. Upon excitation to the quartet state, PtC^+ is expected to promote an electron from one of the nonbonding δ orbitals to an unoccupied π orbital. This transition is calculated to be energetically expensive, and occupation of the antibonding orbital leads to an expected stretching of the Pt−C bond (see Table 2).

PtC_{2n+1}^+. Now consider the case of odd values of x, $3 \leq x \leq 9$. In Figure 4, the interactions of the platinum ion with the frontier orbitals of the respective C_x chain are shown. For odd x, the doublet states are calculated to be considerably more stable than the quartet states. Here, the doublet-quartet transition entails a costly excitation of one of the electrons in the terminal lone pair (orbital C) of the carbon chain to an unoccupied π orbital E of primarily carbon character. Because this transition only involves orbitals on the carbon chain, no change is observed in the Pt−C bond length.

As in the linear C_x chains, changes in orbital occupation are found in the PtC_x^+ clusters with increasing x. It was noted earlier that, as the C_x chain increases in length, more orbitals of π symmetry appear in the frontier region. For odd values of x, Figure 4 can be used to explain the approach to the π continuum via the gradual rise of orbital D with respect to the localized σ orbitals. Also, more π orbitals of similar character will fill in below orbital D. At $x = 11$, orbital D becomes less stable than C for the quartet state, changing the orbital occupation in the quartet state and the nature of the doublet-quartet transition. This excitation now involves the promotion of an electron from a Pt−C π orbital (orbital D) to a π orbital (orbital E) comprised primarily of carbon character. Thus, in the quartet state, a carbon lone pair (orbital C) is double-occupied in favor of a π antibonding orbital (orbital D). It might initially seem peculiar that this causes no significant change in the Pt−C bond length of the quartet state. However, as orbital D rises in energy relative to the lone pairs, it participates in a relatively smaller portion of the net metal−carbon π interaction than it did for shorter carbon chains. In addition, the lowest-energy unoccupied π orbital will likewise become more nonbonding as it approaches the π continuum from above. This is evidenced by the decreasing doublet-quartet splitting energy seen in Figure 1 for odd x and leads to less antibonding character in orbital E. Consequently, the orbital switch at $x = 11$ for the quartet state is not accompanied by a shortening of the Pt−C bond.

For $x \geq 13$ in the quartet state, orbital D is calculated to also become less stable than orbital B. Thus, a change of electron configuration occurs as an electron is switched from orbital D to orbital B. Primarily due to mixing from the platinum atom's low-lying 6s orbital, orbital B exhibits considerable σ-bonding character. Thus, the change in the orbital occupation at $x = 13$ for the quartet state results in an decrease in Pt−C bond length. This ordering of the frontier orbitals is expected to be maintained for larger values of x. For the doublet state, it is not until $x = 15$ that orbital B is calculated to be filled in favor of orbital D. As above, the double occupation of the σ-bonding orbital B leads to a reduction in the Pt−C bond distance.

It is clear from their composition that the orbitals A and B from Figures 3 and 4, respectively, would exhibit very similar characteristics. However, as previously mentioned, orbital B will exhibit considerably more bonding character. It can be seen in Table 2 that changing $x = 1$ to odd $x > 1$ leads to a substantial increase in the Pt−C bond length. Thus, for the case of odd $x > 1$, the antibonding orbital contributions from the carbon lone

Table 3. Energy of the Lone Pair Orbitals in the Doublet State of the Linear C_x Chains

x	σ_u (hartrees)	σ_g (hartrees)	x	σ_u (hartrees)	σ_g (hartrees)
4	−0.361	−0.347	12	−0.316	−0.316
6	−0.340	−0.338	14	−0.312	−0.311
8	−0.329	−0.329	16	−0.308	−0.308
10	−0.322	−0.321			

pair and σ Pt^+ orbitals are less. Orbital B is less destabilized by the antibonding interaction and has an increased bonding character.

PtC_{2n}^+. Now consider the binding energy trends in PtC_x^+ for the case of even x, $2 \le x \le 16$. Invariably, the doublet-quartet transition for these complexes is less energetically costly than for odd x. In fact, the quartet is found to be the most stable species until $x \approx 6$. It can be seen in Figure 5 that the transition involves the promotion of an electron from orbital F to orbital G. In a fashion similar to the previously discussed orbital B, orbital F will have notable σ-bonding character. Also, orbital G will portray negligible π-antibonding character for larger values of x. Thus, the calculated Pt−C bond distances for the quartet state exhibit the expected increase as the metal−carbon bond order is depleted by the promotion of an electron from a bonding orbital (F) to a nonbonding one (G).

Conveniently, the analysis for the PtC_x^+ linear clusters with even x is much less involved than that for the clusters with odd x. This is due primarily to the fact that, in the calculations performed on the systems with even x, no changes in orbital occupations were found. However, for some $x > 16$, it is expected that an occupied π-nonbonding orbital will rise above orbital F in Figure 5, causing a switch in the electron configuration of the quartet states with even x. This alteration will be very much akin to those previously examined, leading most likely to a contraction of the Pt−C bond length to about 1.77 Å.

For linear PtC_x^+ clusters with both even and odd values of x, Figure 1 displays a gradual increase in binding energy as x increases. This increasing Pt−C bond order for even x is attributed to the rising energy of the C_x lone pairs (Table 3). It is clearly seen in Figure 5 that, as the bonding carbon lone pair (labeled "near lone pair") approaches the 5d Pt^+ orbitals in energy, a greater σ interaction will occur. A Mulliken population analysis of this series also indicates that the most rapidly increasing interaction is between the platinum 5d orbitals and the lone pair of the carbon chain. Consequently, an increase in binding energy would be expected with longer C_x chain lengths. An entirely analogous argument holds for the case of odd x, explaining the generally downward slope in Figure 1.

Open-Ring Clusters. Figure 6 portrays the calculated binding energies for the open-ring clusters, $6 \le x \le 16$, relative to the linear C_x chain and platinum cation. In all cases, the doublet state was found to be more stable that the quartet. However, the two states are energetically competitive for the open-ring PtC_x^+ clusters with $x = 4n + 2$. In general, the Pt−C bond lengths (Table 2) are longer than those calculated for the linear clusters. (Note that each open-ring cluster has two equivalent Pt−C bonds.) The metal−carbon bond length remains relatively constant for the doublet state at 1.87−1.90 Å, and the Pt−C bond length in the quartet state is calculated to vary from 1.88 to 1.93 Å.

The bonding of the linear C_x and linear PtC_x^+ clusters provides deep insight into the electronic structure of the open-ring PtC_x^+ clusters. Quite simply, these complexes can be visualized as linear clusters in which the terminal lone pair bends around to interact with the metal atom. A complete bonding description may be obtained by considering the frontier orbitals in the C_x clusters distorted to interact in the fashion of the open-ring clusters.

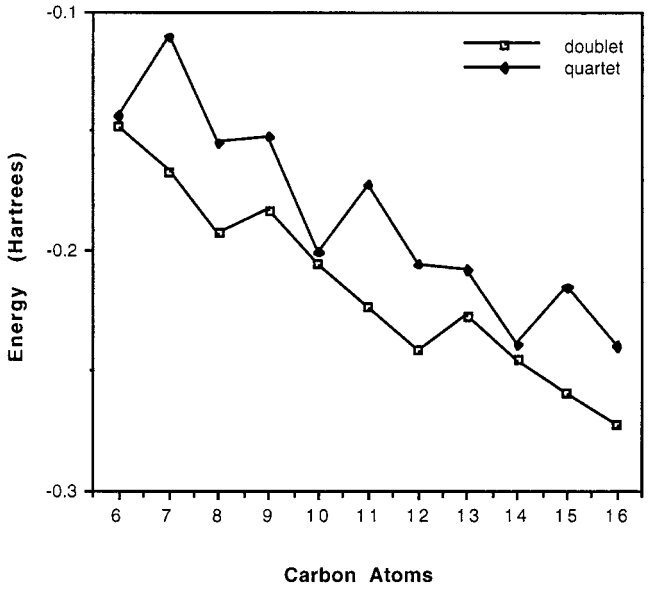

Figure 6. The binding energy of the doublet and quartet states of the open-ring PtC_x^+ clusters with respect to Pt^+ and the corresponding linear C_x chain.

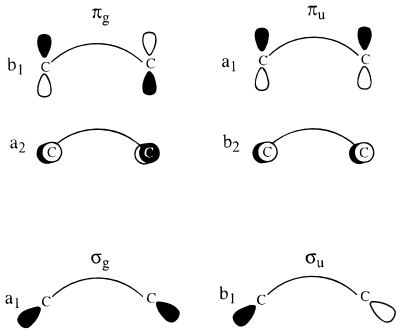

Figure 7. The frontier orbitals of the linear C clusters upon bending of the chain. (Note that the carbon chain is in the plane of the paper.)

The differences in the bonding of the linear and open-ring PtC_x^+ clusters arise from the physical distance between the platinum cation and the endpoints of the respective C_x moieties. In the linear clusters, only one end of the carbon chain interacts significantly with Pt^+. On the other hand, both ends of the C_x chain are close enough in the open-ring clusters to have bonding interactions. Thus, the parity of the orbital contributions from the endpoints of the C_x chain is a factor in the open-ring clusters that did not require consideration in the linear clusters. Figure 7 displays the irreducible representations to which the frontier orbitals of the carbon chains correspond upon distortion from the linear geometry. The figure shows that classification of the frontier π-like orbitals from the carbon chains in C_{2v} symmetry will divide them into four groups. By analogy with the orbitals which lead to Hueckel's rules of aromaticity, a four-carbon "periodicity" may be expected in the bonding trends of the open-ring clusters.

As seen in Figure 6, the binding energy clearly undulates as expected. The rapid increase in binding energy (with respect to Pt^+ and the linear C_x chain) with larger x is primarily due to a reduction in the strain of bending the linear carbon chain to form the open-ring clusters. The long Pt−C bond distances (Table 2) are necessarily connected with less π-bonding in the

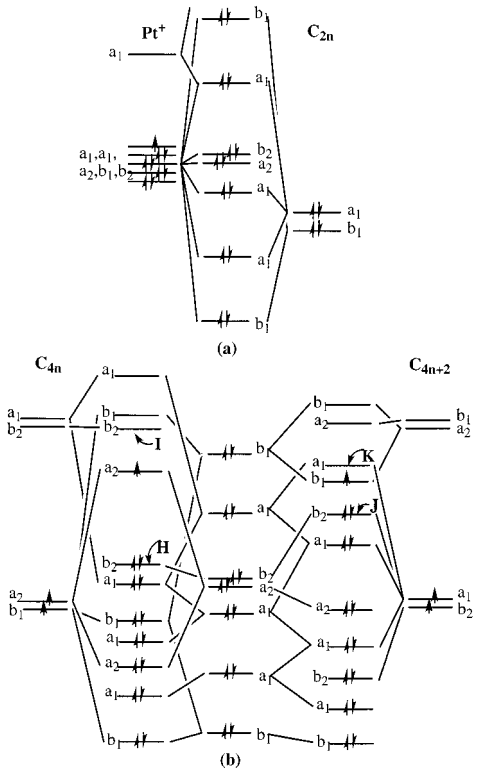

Figure 8. Partial MO diagrams showing the interaction of the platinum cation and bent carbon chain in a open-ring cluster. (a) Only the σ interactions are considered. (b) The π interactions are added to complete the diagram.

open-ring clusters. The π-like orbitals (see Figure 7) will have relatively small overlap with the platinum d orbitals. However, it will be shown that the existing π bonding leads to interesting trends in the doublet-quartet splitting energies.

A particularly obvious trend seen in Figure 6 is that the doublet-quartet splitting is considerably larger for the PtC_x^+ open-ring clusters in which x equals $4n$ than those in which it equals $4n + 2$. (Recall that these splittings were essentially identical in the case of the linear isomers.) It is seen from Figure 2 that for both $x = 4n$ and $x = 4n + 2$, the C_x cluster will contribute two fully occupied σ-like orbitals, two half-filled π-like orbitals, and two unoccupied π-like orbitals to the frontier orbital region. Figure 7 displays the symmetry of these orbitals after the C_x chain has been distorted. The σ bondings for the cases of $x = 4n$ and $x = 4n + 2$ are essentially identical. For clarity, the molecular orbital diagram for the open-ring clusters will be constructed in two steps. First, the interaction of the orbitals of the metal ion with the lone pairs of the C_x clusters can be seen in Figure 8a. One molecular orbital diagram can suffice for $x = 4n$ and $x = 4n + 2$ because the symmetries of the σ-like orbitals are the same for both cases. Differences in the bonding of the two classes appear as a result of the π interactions displayed in Figure 8b. In the completed molecular orbital diagram (Figure 8b), it can be seen that the π-like orbitals on the carbon chains are contrasting for $x = 4n$ and $x = 4n + 2$. Although both cases exhibit an unoccupied pair and a half-filled pair of orbitals, the symmetries of these pairs are switched. Notice that, for the case in which $x = 4n$, the excitation to the quartet state will entail promoting an electron from orbital H to orbital I, a high-energy π orbital located mostly on the carbon chain. However, for the case involving $x = 4n + 2$, a lower energy excitation is available. Orbital K, a metallic orbital exhibiting weak σ and π antibonding character, will fall considerably lower in energy than the excited orbitals located on the carbon chain. Thus, the energy required to excite an electron from orbital H to orbital I will be decidedly more than that required to excite an electron from orbital J to orbital K. This explains the observed trend in Figure 6.

One-Carbon and Closed-Ring Clusters. The bonding in clusters involving a complete carbon ring will be rationalized primarily in terms of the expected Hueckel orbitals. The C_x rings each contain two conjugated systems: one in the plane of the molecule and the other perpendicular to this plane. On the basis of the expectation that these two systems become essentially identical at large x, all of the C_x rings were examined in a spin state where an equal number of electrons occupy the two conjugated systems.

To best model the Pt^+-C_x interaction, we first optimized the geometries of the lone C_x rings with DFT under two constraints. The first is that they would remain planar. The second constraint was that the rings would display a C_2 axis of symmetry coincident with that in the C_x moiety in the associated PtC_x^+ species. Unfortunately, this leads to a complication for the C_x rings with even x. Two nonequivalent C_2 axes are possible for each ring:

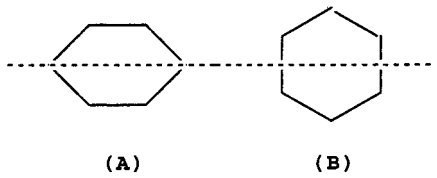

These are best visualized in terms of the respective C_2 axes of the one-carbon and closed-ring PtC_x^+ clusters. In the cases where nonequivalent C_2 axes simultaneously exist, we simply calculated both possible C_x structures and separately utilized them where appropriate. In general, examination of the one-carbon PtC_x^+ clusters with even x will be with respect to (A), whereas (B) will be employed for the corresponding closed-ring structure. At most, we found the energies of (A) and (B) to differ by less than 3.7 kcal mol^{-1}.

The aforementioned assumptions are by no means flawless. For example, we found that the C_7 ring favors a triplet spin state with both unpaired electrons in the plane of the molecule. Also, frequency calculations[21] have shown that the ground-state geometry of many C_x rings with even x do not have C_{2v} symmetry. However, deviation from these approximations has been found to be subtle and highly method-dependent.[23] The description of the metal−carbon interaction and the nature of the bonding trends will not be affected.

Figures 9 and 10 exhibit the binding energy of the one-carbon and closed-ring PtC_x^+ clusters with respect to the Pt^+ cation and the C_x carbon ring. The Pt−C bond lengths are displayed in Table 4. Both groups of clusters are most weakly bound for the case of $x = 4n + 2$, and the doublet-quartet splitting energies are greatest for $x = 4n + 2$ and $x = 4n + 3$. The binding energies of the doublet states are calculated to increase substantially for the cases of $x = 4n + 3$ and $x = 4n$ in both the one-carbon and closed-ring clusters. As seen in Table 4, the length of the Pt−C bond in the one-carbon clusters undergoes dramatic oscillations as the number of carbon atoms is increased. For the doublet state, the Pt−C bond is longest in the one-carbon PtC_x^+ clusters when $x = 4n + 2$, and it is shortest when $x = 4n$. Conversely, the two equivalent Pt−C bonds in the closed-ring clusters remain essentially constant for all calculated values of x (Table 4). The Pt−C bonds are 1.95−1.99 Å in the doublet states and 1.96−1.98 Å in the quartet states of the closed-ring clusters.

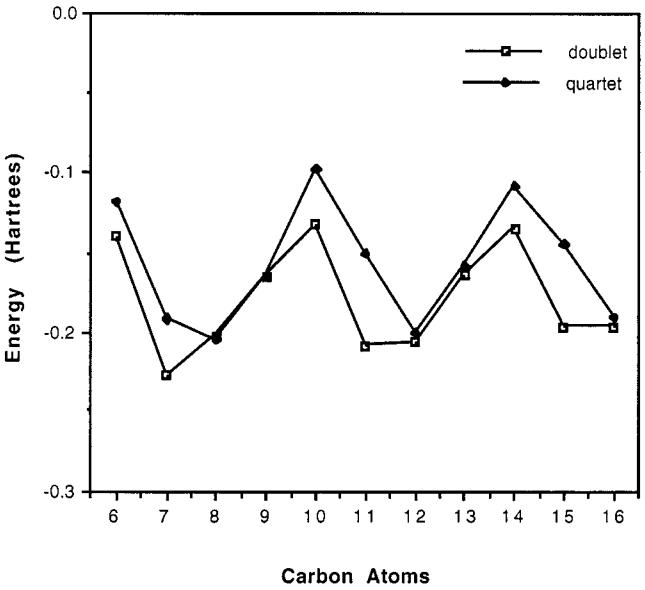

Figure 9. The binding energy of the doublet and quartet states of the one-carbon PtC_x^+ clusters with respect to Pt^+ and the corresponding C_x ring.

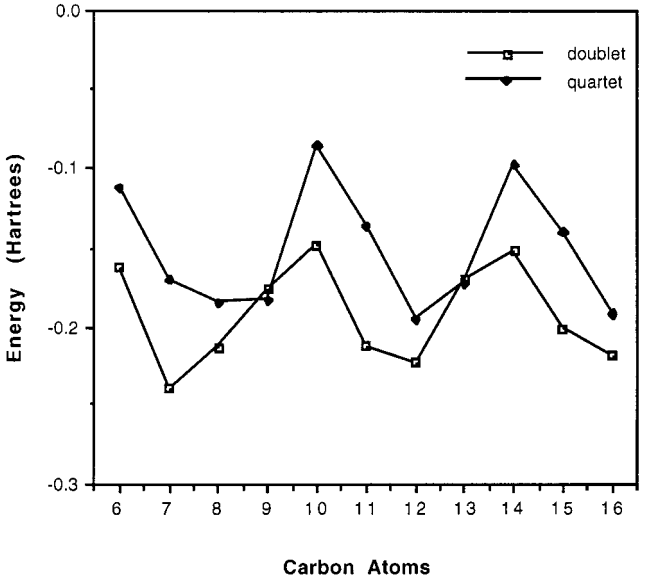

Figure 10. The binding energy of the doublet and quartet states of the closed-ring PtC_x^+ clusters with respect to Pt^+ and the corresponding C_x ring.

The periodicity displayed in the Figures 9 and 10 immediately suggests that the aromaticity of the carbon rings is a large factor in the nature of the Pt^+-C_x bonding. For $x = 4n + 2$ (the case of maximum aromaticity), the planar C_x moiety would be relatively stable unto itself and have little to gain from an interaction with the platinum cation. For $x = 4n$, however, the antiaromatic C_x ring would be driven toward the relief afforded by an interaction with the metal. Electron density obtained from the π-like orbitals of the platinum cation would make the C_x ring more aromatic in character. These hypotheses are supported for the one-carbon clusters by spin density data presented in Figure 11. Note that, for the doublet case of $x = 6$ ($x = 4n + 2$), the Pt−C bond distance is 1.95 Å and the radical electron is primarily located on the platinum cation. This indicates a minor interaction between the closed shell C_x ring and the radical metal cation. However, a stronger bond is found for $x = 8$ ($x = 4n$), in which the bond distance contracts to 1.84 Å. The spin

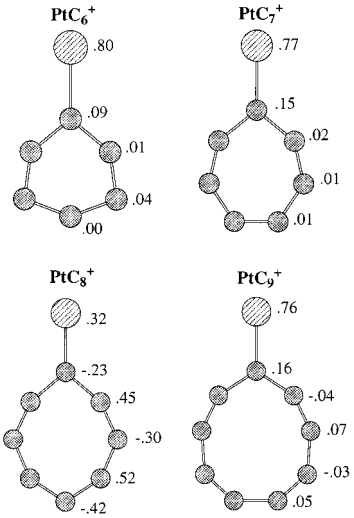

Figure 11. Spin density localized to each atom in the PtC_x^+ one-carbon clusters, $6 \leq x \leq 9$.

Table 4. Pt−C Bond Length in the Doublet and Quartet States of the One-Carbon and Closed-Ring PtC_x^+ Clusters

	one-carbon		closed-ring	
x	doublet (Å)	quartet (Å)	doublet (Å)	quartet (Å)
6	1.95	1.90	1.95	1.96
7	1.88	1.96	1.96	1.97
8	1.84	1.88	1.96	1.96
9	1.88	1.92	1.99	1.96
10	1.97	1.91	1.96	1.97
11	1.90	1.98	1.97	1.97
12	1.86	1.90	1.97	1.98
13	1.90	1.93	1.99	1.97
14	1.97	1.92	1.97	1.98
15	1.91	1.99	1.98	1.97
16	1.87	1.91	1.98	1.98

Table 5. Mullican Charge of the Platinum Atom in the Doublet State of the One-Carbon Clusters

carbon atoms	charge of Pt atom	carbon atoms	charge of Pt atom
6	0.725	12	0.524
7	0.654	13	0.651
8	0.601	14	0.591
9	0.720	15	0.554
10	0.794	16	0.465
11	0.598		

density suggests that the radical electron is distributed throughout a π-orbital composed of contributions from both the platinum atom and the carbon-ring system. In general, it appears that the platinum cation is behaving as an "electron-sink." That is, the relatively accessible electrons on the metal atom may be utilized to maximize the aromatic character of conjugated system on the C_x moiety. Table 5 clearly shows that the platinum atom donates electron density to the carbon ring in this fashion. In general, the Mulliken charge on the platinum atom displays local maxima at $x = 4n + 2$ and local minima at $x = 4n$. These conclusions will now be examined from a somewhat more rigorous standpoint.

Figure 12 exhibits MO diagrams of the one-carbon PtC_x^+ clusters for the cases $x = 4n + 2$ and $x = 4n$. Comparison of the two cases provides insight into their relative binding energies. Note that, for $x = 4n + 2$, the high-energy π orbitals on the C_x ring are unable to contribute much to a stabilizing interaction with the orbitals of the platinum cation. In addition, the relatively large doublet-quartet excitation energy observed

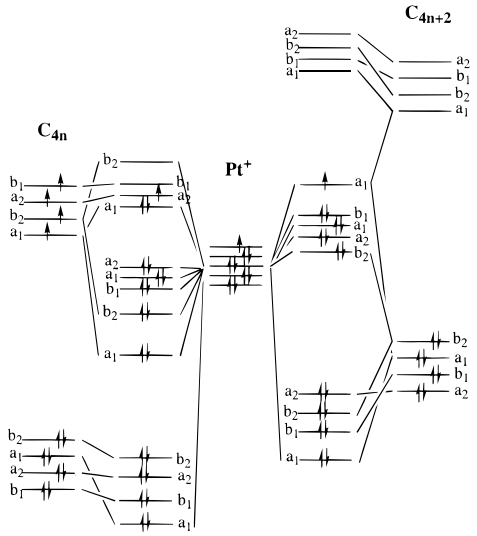

Figure 12. Partial MO diagrams showing the interaction of the platinum cation and carbon ring in a one-carbon cluster.

in Figure 9 is explained by the need to promote an electron into these unstable π orbitals. On the other hand, the respective π orbitals in the case of $x = 4n$ are considerably lower in energy. These orbitals have been partially occupied by electrons from the carbon chain and now readily participate in stabilizing interactions with the metal cation. The relatively short Pt−C bond length for the $x = 4n$ series of one-carbon clusters (see Table 4) is directly attributed to the stability obtained from the overlap of the metal and C_x orbitals. In addition, the doublet-quartet excitation energy now only requires the transfer of an electron among nearly degenerate π orbitals. This is seen in Figure 9 to be a low-energy, and sometimes favorable, transition.

Analysis of the closed-ring species yields results that are generally similar to those for the one-carbon clusters above. However, the Pt−C bond length of the closed-ring systems (see Table 4) does not exhibit the same dramatic alternations with increasing C_x ring size. This constancy in the bond length is due to fact that the C−Pt−C bond angle is critical to maximizing a favorable orbital interaction. Maintenance of a constant bond angle prevents the closed-ring clusters from displaying the facile bond-length alternations observed in the one-carbon clusters.

Comparison of Structural Families. In light of the fact that the electronic structures of the closed-ring and one-carbon cluster are so similar, it is interesting to consider which is generally more stable. Table 6 indicates that the closed-ring clusters invariably have lower energy. The geometry of the closed-ring systems enables a larger (more σ-like) interaction between the orbitals of the carbon ring and two of the platinum cation's d orbitals, whereas the one-carbon clusters only exhibit such an interaction for one d orbital. Essentially, the two σ bonds of the platinum closed-ring species are stronger than the σ bond and π bond exhibited by the one-carbon PtC_x^+ clusters. Such is not invariably the case for the isoelectronic PdC_x^+ systems[35] in which the more stable species depends on the value of x. As discussed previously for the PtC_2^+ fan structure, the metal component in the σ bonds of the closed-ring clusters is mostly comprised of sd hybrid orbitals. The greater stability of the closed-ring structures is based on the fact that the 6s orbital on the metal atom is considerably lower in energy for platinum than for palladium. The lower-energy sd hybrids favor the formation of two σ bonds, and thus, the PtC_x^+ closed-ring species are more readily formed.

Table 6. Energy of the Doublet States Relative to the Linear PtC_x^+ Clusters

x	linear (kcal mol^{-1})	open-ring (kcal mol^{-1})	one-carbon (kcal mol^{-1})	closed-ring (kcal mol^{-1})
6	0.00	21.97	50.60	38.25
7	0.00	13.35	35.37	27.61
8	0.00	3.19	49.22	41.91
9	0.00	9.77	51.27	45.03
10	0.00	2.31	3.17	−4.35
11	0.00	−11.18	−5.32	−7.67
12	0.00	−15.06	11.58	1.76
13	0.00	−9.01	10.36	6.28
14	0.00	−12.67	−15.59	−22.54
15	0.00	−25.48	−23.93	−26.90
16	0.00	−26.06	−8.03	−19.39

As seen for the palladium−carbon cations,[35] the nonlinear PtC_x^+ systems are favored for $x \geq 10$ (Table 6). With the increasing number of carbon atoms, the strain of ring formation becomes less prohibitive. Recall that shortcomings in the carbon basis set may lead to the overestimation of the ring strain in the nonlinear species. The open-ring systems, which are not subject to the aforementioned aromaticity effects, are calculated to be the most stable species for $x = 4n$, $x \geq 10$. However, for $x = 4n + 2$ and $x \geq 10$, the closed-ring systems are the lowest in energy.

Acknowledgment. We thank the National Science Foundation (Grant Nos. CHE 94-23271, CHE 98-00184, and CHE 95-28196) and the Robert A. Welch Foundation (Grant No. A-648) for financial support.

JA990854N